

# Advances in Hybrid Molecular/Continuum Methods for Micro and Nano Flows

Matthew K. BORG<sup>1</sup>, Duncan A. LOCKERBY<sup>2</sup>, Jason M. REESE<sup>3,\*</sup>

\* Corresponding author: Tel.: +44 (0)131 651 7081; Email: jason.reese@ed.ac.uk

1: Department of Mechanical & Aerospace Engineering, University of Strathclyde, Glasgow, UK

2: School of Engineering, University of Warwick, Coventry, UK

3: School of Engineering, University of Edinburgh, Edinburgh, UK

**Abstract** Next generation fluid flow systems are likely to depend on micro or nano scale dynamics that make the system behaviour multiscale in both space and time. There may be strong or weak separation between the length scales and between the time scales in different parts of the flow, and these scale-separations may also vary in space and time. In this paper we discuss a practical approach to improving the efficiency of hybrid particle/continuum models of such multiscale flows. Our focus is on adapting the solution method to the local scale-separation conditions, in order to balance computational efficiency with accuracy. We compare results from our new hybridisation in space and time with full molecular simulations of benchmark nanoscale flows.

**Keywords:** hybrid methods, micro flows, nano flows, molecular dynamics, scale separation.

## 1 Introduction

Conventional continuum fluid dynamics can be a poor predictor of flows at the nano scale (for liquids) or the micro scale (for gases). This is because atomistic processes occurring over pico or nano scales determine bulk fluid effects occurring over micro and milli scales, both temporally and spatially. While Molecular Dynamics (MD) can resolve fluid behaviour at the smallest space and time scales, its high computational cost deters its widespread adoption.

However, a major feature of micro and nano scale devices is that fluids often flow within long channel or pipe structures, e.g. micro heat exchanger pipes, nanotubes, etc. The length-scale-separation between hydrodynamic processes occurring along the direction of the flow, and molecular processes occurring on scales transverse to the flow direction could be exploitable by a hybrid method that partitions the flowfield between a molecular solver and a continuum-fluid solver. If the flow is unsteady or transient there may also be a disparity in time-scales that a hybrid solver could exploit to make performance gains. In this paper we present such

a coupling of molecular and continuum solvers concurrently in one simulation. Computational speed-up over full scale molecular simulations is obtained by exploiting scale-separation in both time and space.

## 2 Method

The Internal-flow Multiscale Method (IMM) of Borg et al. [1] and Patronis et al. [2], which was developed to deal with steady liquid and gas flows, respectively, is extended here to simulate transient/unsteady flow. The algorithm is posed in the time-stepping coupling framework described by Lockerby et al. [3].

### 2.1 Scale-separation

Consider a channel of gradually varying cross-sectional height  $h$ , as shown in fig. 1(a), where a length-scale-separation

$$S_L(s) = \left| \frac{dh(s)}{ds} \right|^{-1}, \quad (1)$$

exists in the direction  $s$  parallel to the flow, but there is no such scale-separation in the direc-

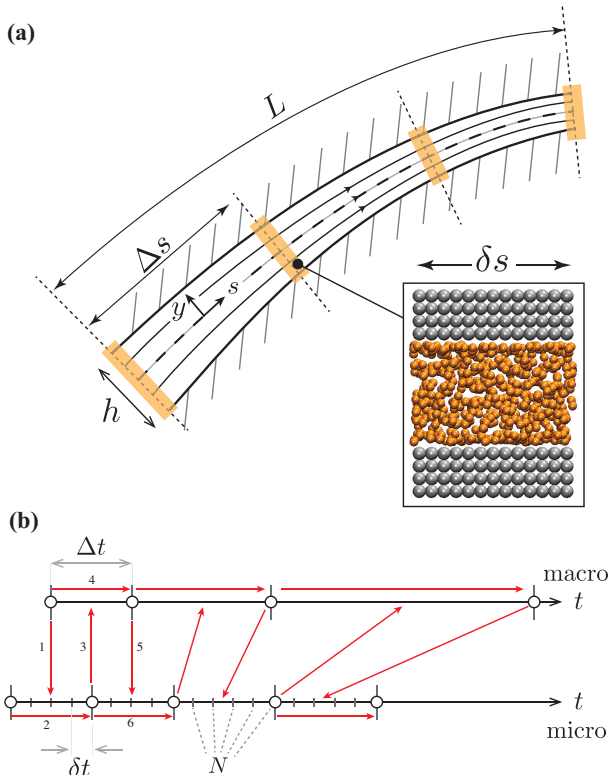


Figure 1: Schematic of hybrid framework decomposition for: (a) length-scales (showing a representative MD micro element), and (b) time-scales.

tion  $y$  perpendicular to the flow direction. Provided  $S_L \gg 1$  (as is the case in high aspect ratio channels)<sup>1</sup> it can safely be assumed that, in small streamwise sections of the channel, the walls are approximately parallel to the centre streamline. This is a *local parallel-flow assumption*, and it enables the representation of small sections of the channel geometry by micro sub-domains with exactly parallel walls and common periodicity applied in the streamwise direction; a convenient setup for MD ensembles. The ratio of continuum to molecular sub-domain sizes,  $g_L = \Delta s / \delta s$ , is an indication of the amount of computational speed-up gained over a full molecular calculation.

In the case of time-varying problems, a further computational gain can be obtained if a time-scale-separation

$$S_T(t) = \frac{T_{\text{macro}}(t)}{T_{\text{micro}}}, \quad (2)$$

<sup>1</sup>See Ref. [4] for cases treated when  $S_L(y) \gg 1$  and Ref. [5] for cases treated when  $S_L(s) < 1$  in some parts of the channel.

exists between macroscopic ( $T_{\text{macro}}$ ), and microscopic ( $T_{\text{micro}}$ ) time-scales. In this relationship  $T_{\text{macro}}$  is the time scale characterising the temporal variation  $t$  in the macro variables (e.g. the period of an oscillatory flow) and  $T_{\text{micro}}$  is the characteristic time needed for the variables in the micro model to relax after any step change in macro variables (e.g. a start-up time from rest).

From a numerical perspective, time is inherently discretised using time-steps  $\Delta t$  and  $\delta t$  for the macro and the micro solvers respectively. The maximum time-step size which is allowed for the MD solver is based entirely on stability, and is taken to be  $\delta t = 5$  fs for all cases in this paper. For a macroscopic solver the time-step is expressed as

$$\Delta t = \frac{T_{\text{macro}}}{n_{\text{macro}}}, \quad (3)$$

where  $n_{\text{macro}}$  is a large value that: a) captures the macroscopic temporal variation of the hydrodynamic properties, b) satisfies the numerical CFL condition, and c) assures the hybrid simulation is stable. We note that  $\Delta t$  may vary depending on temporal macroscopic variations,  $T_{\text{macro}}(t)$ , and hence  $S_T(t)$ . This means that we need a generalised time-stepping procedure for the macro and micro time-scales throughout the hybrid simulation that allows this variability on-the-fly. We therefore adopt the *Continuous micro solution-Asynchronous, Intermittent coupling* (CAI) time-stepping method of Lockerby et al. [3].

In CAI, the micro and macro time-scales are effectively decoupled — which can be visualised as running the macro and micro simulations on two different clocks (or time-lines), as illustrated in fig. 1(b). A micro interval consists of  $N$  MD time-steps (i.e.  $N\delta t$ ), while a macro interval consists of one macro time-step  $\Delta t$ . Micro $\leftrightarrow$ macro exchange of information during the hybrid simulation will occur at these intervals. An indication of the computational speed-up gained through the CAI time-stepping method over a fully-coupled time-stepping procedure (i.e. when  $\Delta t = N\delta t$ ) can be obtained using a micro gearing parameter for time:  $g_T = \Delta t / N\delta t$ . Computational savings are obtained when  $g_T > 1$ .

In general this temporal gearing is allowed to adapt throughout the simulation depending on the local value of  $S_T$ . In order to enable this, a relationship between  $g_T$  and  $S_T$  has to be estab-

lished, which is proposed in [3] as:

$$g_T = k_g(S_T - 1) + 1, \quad (4)$$

where  $k_g$  is a proportional gain that acts as a control on how aggressively scale-separation is exploited at the expense of accuracy. When  $k_g = 0$ , we obtain no gearing ( $g_T = 1$ ), and so there is no computational speed up (a reasonable choice for  $S_T \approx 1$  throughout the simulation). For  $S_T > 1$ ,  $k_g$  can be chosen to determine the required level of temporal gearing  $g_T$ .

By substituting the definition of  $g_T$  in Eqn. (4) we can also obtain  $N$  as it adapts during the simulation depending on the scale-separation:

$$N = \frac{\Delta t}{\delta t[k_g(S_T - 1) + 1]}. \quad (5)$$

## 2.2 Coupling

To describe our Micro $\leftrightarrow$ macro coupling methodology, let a hybrid system be represented by the coupled macro and micro equations:

$$\frac{\partial U}{\partial t} = W(U; \gamma(u)), \quad [\text{macro}] \quad (6)$$

$$\frac{\partial u}{\partial t} = w(u; \Gamma(U)), \quad [\text{micro}] \quad (7)$$

with initial conditions

$$U = U^0, \quad \text{and} \quad u = u^0, \quad (8)$$

where  $u$  are the micro variables (e.g. molecular positions and velocities in all MD sub-domains),  $U$  are the macro fluid variables, and the operators  $W$  and  $w$  represent the macro and micro models respectively. The operators  $\Gamma$  and  $\gamma$  represent models, defined later, for processing variables passed between the macro and micro models. The superscript denotes a time index.

For an isothermal flow, the macro model consists of the unsteady, compressible, mass continuity equation. For local parallel flow, this can be written as

$$\frac{\partial \rho}{\partial t} + \frac{1}{A} \frac{\partial \dot{m}}{\partial s} = 0, \quad (9)$$

where  $\dot{m}(s, t)$  is the mass flow rate,  $A(s)$  is the cross-sectional channel area, and  $\rho(s, t)$  is the mass density. The mass flow rate in Eqn. (9) is supplied by the MD sub-domains, i.e.  $\dot{m} = \gamma(u)$  at every coupling interval.

The conservation of momentum must also hold at both macro and micro scales. We use the unsteady, compressible, momentum equation of viscous flow, which can be written for local parallel flow as :

$$\rho \frac{\partial v_s}{\partial t} = -\frac{\partial p}{\partial s} + \nabla \cdot \mathbb{T} + F_s. \quad (10)$$

where  $v_s$  is the velocity in the streamwise direction,  $p$  is the hydrostatic pressure,  $\mathbb{T}$  the shear stress tensor, and  $F_s$  is a source of flow in terms of force per unit volume.

The momentum balance for parallel-wall MD sub-domains with periodicity in the streamwise direction cannot support a streamwise pressure gradient, and so the term  $-\partial p/\partial s$  in Eqn. (10) is missing in the momentum balance of each sub-domain. To produce the hydrodynamically equivalent effect of the missing local pressure gradient in the micro model, an artificial body force  $\Phi$  — the *pressure gradient correction* — is applied as an external forcing to the governing equations of motion of the MD molecules,

$$\mathbf{f}^{\text{ext}} = \hat{\mathbf{n}}_s \frac{F_s}{\rho_n} + \hat{\mathbf{n}}_s \frac{\Phi}{\rho_n}, \quad (11)$$

where  $\rho_n$  is the number density and  $\hat{\mathbf{n}}_s$  is the unit vector local to the sub-domain pointing in the streamwise direction. The macro-to-micro coupling is therefore  $\Phi = \Gamma(U) = -\partial p/\partial s$ .

Finally, to close the set of equations, an equation of state is required to relate the density  $\rho$  in the continuity equation (9) to the pressure in the momentum balance. We formulate this equation of state from the MD sub-domains as outlined in [6].

## 3 Results

We now apply our hybrid method to a periodic converging-diverging channel geometry, which has a smoothly varying height in the streamwise direction. A gravity-type force generates an unsteady/transient flow of a Lennard-Jones fluid inside the channel. All the MD properties we use are described in Ref. [5].

A full MD simulation of this channel (for validation purposes) is shown in fig. 2(a). It has a length  $L=68$  nm in the streamwise direction  $s$ , a depth of  $\Delta z=5.44$  nm, and heights of 3.4 nm and 2.04 nm at the inlet and throat sections,

respectively. The channel is periodic in both the streamwise and spanwise directions. The cross-channel distance between the upper and the lower walls  $h(s)$  varies in the streamwise direction according to a sinusoidal function:

$$h(s) = 2a \left[ \cos \left( \frac{2\pi s}{L} \right) - 1 \right] + h_{\text{inlet}}, \quad (12)$$

where  $4a=1.36$  nm is the total change of height from inlet to throat, and  $h_{\text{inlet}}$  is the inlet height. The length-scale-separation in the streamwise direction,  $S_L(s)$  is obtained from Eqn. (1), and for this configuration is  $\sim 16$  at the least scale-separated location.

In both the full MD and hybrid simulations the fluids start at rest with the same spatial density distribution  $\rho(s)$ . A time-varying gravity force  $F_g(t)$  is then applied. Four types of time-scale-separated flows are simulated (see Figure 3):

- A. **No scale-separation.** A startup flow problem that applies instantaneously to the fluid a gravity-type body force of  $F_g = 0.487$  pN.
- B. **Weak scale-separation,**  $S_T = 2$ . An unsteady sinusoidal oscillating gravity-type force with amplitude  $F_g = 0.487$  pN and period of  $T_{\text{macro}} = 0.22$  ns.
- C. **Strong scale-separation,**  $S_T = 100$ . An unsteady sinusoidal oscillating gravity-type force of the same amplitude, but with a larger period of  $T_{\text{macro}} = 10.8$  ns.
- D. **Mixed scale-separation,**  $S_T = 2 \rightarrow 100$ . An unsteady oscillating gravity-type force with the same amplitude but with increasing sinusoidal period:  $0.2 \rightarrow 10.8$  ns.

Resolving the converging-diverging channel with micro sub-domains is shown in fig. 2(b). It consists of  $\Pi = 5$  micro elements distributed uniformly at streamwise locations:

$$s_i = L(i - 1)/\Pi, \quad (13)$$

where  $i = 1, 2, \dots, \Pi$  are the indices of the micro elements. A dependency study of  $\Pi$  on numerical accuracy has already been reported in [1, 2], and so is not repeated here. The channel heights of each micro element are a mapping from the macro domain geometry, which

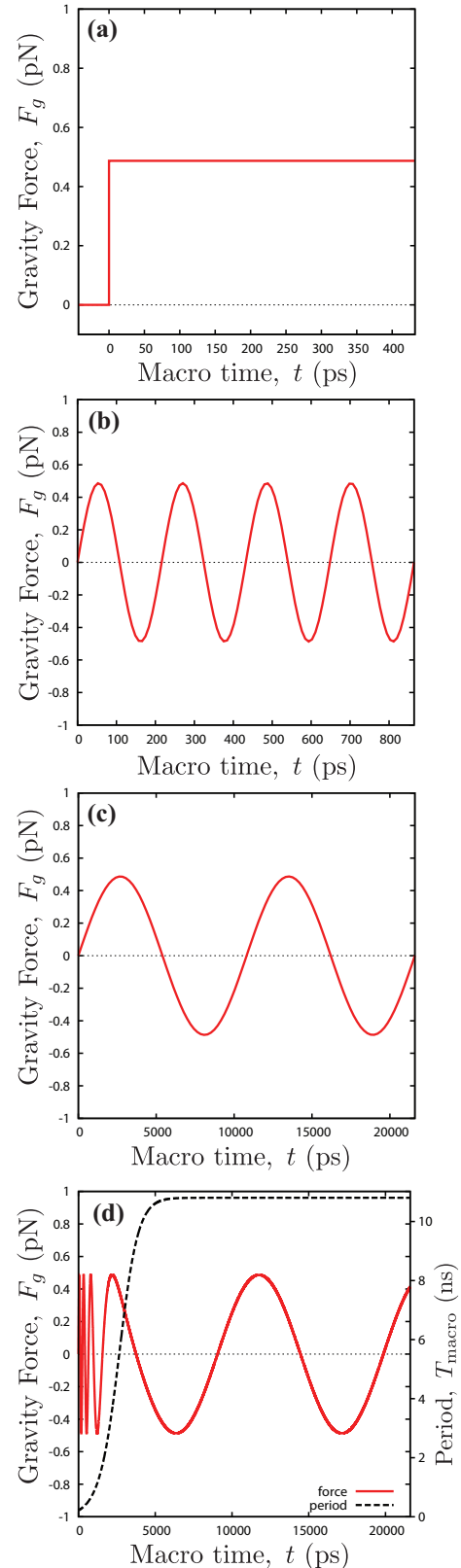


Figure 3: Gravity-type forcing against time for various time-scale-separated cases: (a) startup flow, (b) oscillating force with weak scale-separation  $S_T = 2$ , (c) oscillating force with strong scale-separation  $S_T = 100$  and (d) oscillating force with mixed scale-separation  $S_T = 2 \rightarrow 100$ .

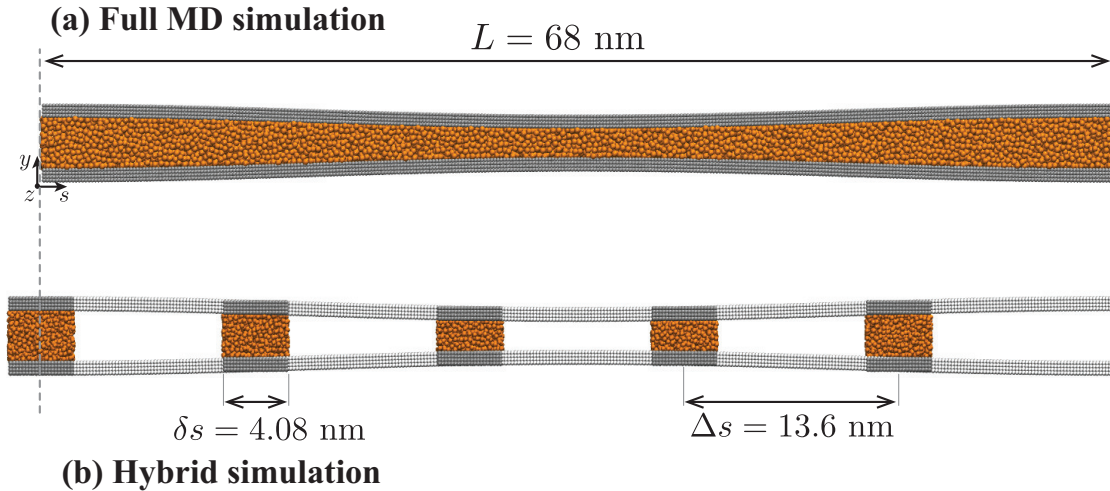


Figure 2: Converging-diverging channel test case (a) full MD simulation, and (b) hybrid continuum/molecular simulation with MD elements illustrated.

can be obtained by substituting the subdomain locations  $s_i$  (Eqn. 13) into the channel's geometry, Eqn. (12). In the streamwise direction all micro elements have an extent  $\delta s = 4.08$  nm, which gives a micro subdomain separation (macro spacing) of  $\Delta s = 13.6$  nm and a computational speed-up estimate due to spatial gearing of  $g_L = 3.33$ . Table 1 gives an overview of the three time-scale-separated cases considered with increasing time gearing  $g_T$ , and the equivalent values of the coefficient  $k_g$ .

| Case B |       | Case C |       | Case D     |       |
|--------|-------|--------|-------|------------|-------|
| $g_T$  | $k_g$ | $g_T$  | $k_g$ | $g_T$      | $k_g$ |
| 1      | 0     | 10     | 0.09  | 1.1–11.1   | 0.1   |
| 2      | 1.0   | 20     | 0.19  | 1.25–20.83 | 0.2   |
| 4      | 3.0   | 40     | 0.39  | 1.43–35.71 | 0.33  |

Table 1: The micro gearing  $g_T$  and the scale-separation coefficient  $k_g$  for the various cases considered.

In order to improve the statistical measurements, and hence the stability of our hybrid algorithm, 10 statistically independent realisations are taken of each micro element. Mass flow rate measurements taken from each micro interval  $N\delta t$  are therefore further averaged across 10 ensembles<sup>2</sup>. However, due to computational

limitations, our full MD simulations were too expensive to be repeated 10 times. Results for the full-MD simulations, which are presented in the following figures, are only from one simulation run and so are noisier than the hybrid solution.

In figs. 4(a)-(d) we show the results for mass flow rates varying in time for the four cases A-D, respectively. For convenience, only the results for the inlet MD subdomain of the converging/diverging channel (i.e.  $i=0, s=0$ ) are plotted; the results for other subdomain locations are qualitatively similar, and so are not presented here. In cases A and B (figs. 4(a) and (b), respectively) the hybrid solution matches quite well with the full-MD solution when  $g_T=1$  (no gearing). In these cases the time-scale-separation is weak ( $S_T \leq 2$ ), and so computational savings cannot be obtained without loss of accuracy. To demonstrate this, we perform hybrid simulations with different values of  $g_T$ . Figures 4(a) and (b) show qualitatively that for weak scale-separated cases the time-accuracy of the solution is sensitive to  $g_T$ . Figure 5 shows the percentage error between the values of the peak mass flow rates produced by the full MD and the hybrid procedures. For example, for case B, fig. 4(b), a change of gearing from  $g_T = 1$  to  $g_T = 2$  produces a  $\sim 30\%$  error in the peak mass flow rate, and a 60% error when  $g_T=4$ .

For case C the scale-separation is much stronger ( $S_T = 100$ ), and so the sensitivity of the solution to  $g_T$  will be much less, as shown qual-

<sup>2</sup>Note: for cases A and B we choose  $N = 10$ , while for case D,  $N$  adapts according to Eqn. (5).

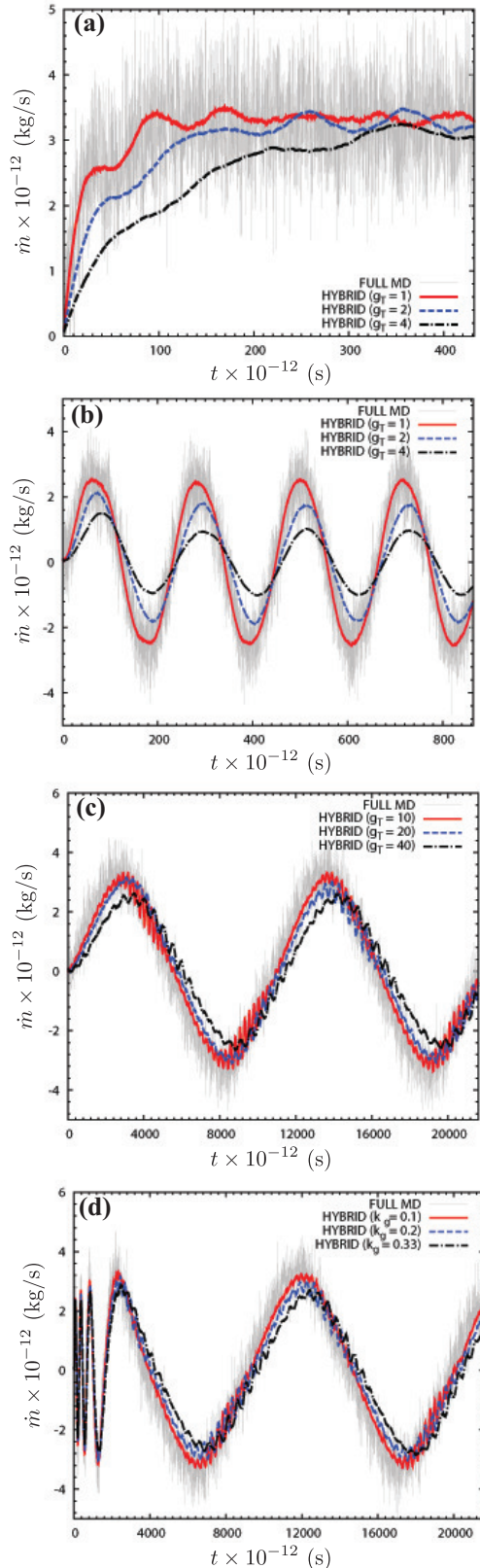


Figure 4: Mass flow rate ( $\dot{m}$ ) variation with time ( $t$ ) at the inlet part of the converging/diverging channel ( $s = 0$ ) for all four test cases — from top to bottom, A–D. Comparison of the hybrid method (with different values of  $g_T$ ) to a full MD simulation.

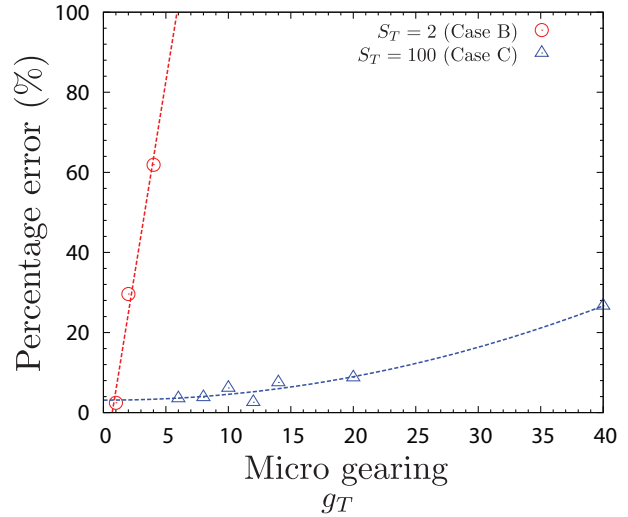


Figure 5: Percentage error of the peak mass flow rate values for the oscillating flow cases B and C, when our hybrid results are compared to the full MD solution.

itatively in fig. 4(c) and quantitatively in fig. 5. Clearly, a reasonable accuracy ( $<10\%$  error) can be achieved in this case for  $g_T < 20$ .

Case D demonstrates the full applicability of the hybrid scheme, as the time-scale-separation  $S_T(t)$  is now a function of time. As such, the gearing parameter  $g_T(t)$  adapts on-the-fly to  $S_T(t)$ . Figure 4(d) clearly shows that the hybrid simulations give excellent results across the range of scale-separation, resolving the initial high frequencies of the flow very accurately using a small gearing, and the lower frequencies of the flow using a higher gearing.

The primary motivation for adopting a hybrid scheme is to obtain accurate results with less computational effort than a full MD simulation. The computational speed-up of our simulations is obtained by dividing the total time-spent for the full MD simulation ( $t_{\text{comp}}^{\text{F}}$ ) by the time taken for the corresponding hybrid simulation ( $t_{\text{comp}}^{\text{H}}$ ), i.e.  $(t_{\text{comp}}^{\text{F}}/t_{\text{comp}}^{\text{H}})$ . The speed-ups of all the cases are shown in fig. 6. In order to make a fair comparison, the computational time for the full MD and the hybrid simulations have been normalised by the number of allocated processors (i.e. as if all the molecules in each approach are run on one processor), as well as by the processing time required to reach the same level of noise.

Naturally, the computational speed-up is

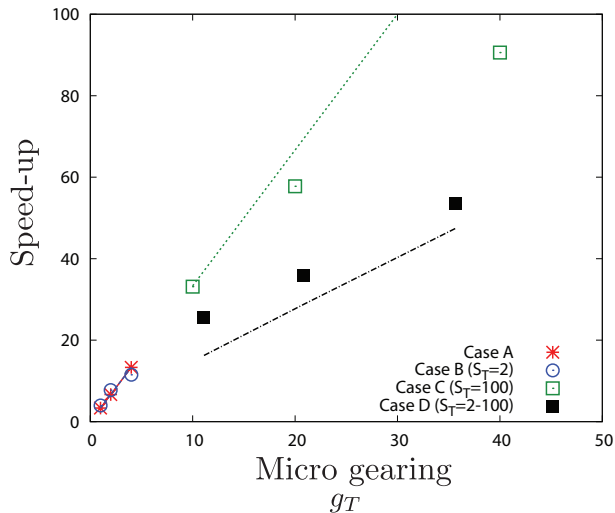


Figure 6: Speed-up (over a full MD simulation) against micro gearing for cases A–D. Symbols denote exact speed-up measurements taken from processor clock times; dashed lines represent an estimation of the speed-up given by  $g_L \times g_T$ . Note that case D has a variable gearing, and in this plot we select the largest gearing.

modest for cases where the accuracy is more sensitive to the micro gearing  $g_T$ , such as cases A and B. However, a sizeable speed-up can be obtained for the strongly scale-separated cases: about  $90\times$  speed-up for case C and  $60\times$  for case D. Note that one should balance the savings (fig. 6) with the level of accuracy required<sup>3</sup> (e.g. fig. 5) to achieve a compromise. The ability to apply numerical gearing is an important feature of the hybrid method here, and it is one which cannot be exploited in a full MD approach.

## 4 Conclusions

We have presented a new hybrid continuum-molecular method that has been developed to deal with compressible, transient flow problems in geometries of large aspect ratio. In these confined geometries, there is strong length-scale-separation in the streamwise direction and no scale-separation in the direction normal to the bounding walls. To resolve the local geometry we apply parallel wall MD micro sub-domains

<sup>3</sup>In practice, when a full MD solution is too costly to obtain as a reference, the accuracy of a hybrid result could be established by running spatial and temporal gearing independence studies.

that are spatially distributed along the domain. The MD simulations are coupled to a set of mass and momentum conservation equations that describe the macroscopic flow in the entire channel; the MD realisations provide a direct local flux refinement to the continuum formulation. As the flow is time-varying, further computational savings can be made by exploiting time-scale-separation. Our hybrid method was validated by comparison to a full MD simulation of a converging/diverging channel with various transient and time-varying flows. The computational speed-up varies across the flow cases we have examined, but we expect speed-ups to be higher for problems with stronger scale-separations.

## Acknowledgments

This work is financially supported in the UK by EPSRC Programme Grant EP/I011927/1, and EPSRC grants EP/K038664/1 and EP/K038621/1. Our calculations were performed on the high performance computer ARCHIE at the University of Strathclyde, funded by EPSRC grants EP/K000586/1 and EP/K000195/1.

## References

- [1] M. K. Borg, D. A. Lockerby, and J. M. Reese. A multiscale method for micro/nano flows of high aspect ratio. *Journal of Computational Physics*, 233:400–413, 2013.
- [2] A. Patronis, D. A. Lockerby, M. K. Borg, and J. M. Reese. Hybrid continuum-molecular modelling of multiscale internal gas flows. *Journal of Computational Physics*, 255:558–571, 2013.
- [3] D. A. Lockerby, C. A. Duque-Daza, M. K. Borg, and J. M. Reese. Time-step coupling for hybrid simulations of multiscale flows. *Journal of Computational Physics*, 237(344–365), 2013.
- [4] M. K. Borg, D. A. Lockerby, and J. M. Reese. Fluid simulations with atomistic resolution: a hybrid multiscale method with field-wise coupling. *Journal of Computational Physics*, 255:149–165, 2013.

- [5] M. K. Borg, D. A. Lockerby, and J. M. Reese. A hybrid molecular-continuum simulation method for incompressible flows in micro/nanofluidic networks. *Microfluidics and Nanofluidics*, 15(4):541–557, 2013.
- [6] M. K. Borg, D. A. Lockerby, and J. M. Reese. The FADE mass-stat: a technique for inserting or deleting particles in molecular dynamics simulations. *The Journal of Chemical Physics*, 140:074110, 2014.